Late Holocene Earthquake History of the Imperial and Brawley Faults, Imperial Valley, California

Aron J. Meltzner and Thomas K. Rockwell

Geological Sciences
San Diego State University

Final Technical Report

U.S. Geological Survey Grant No. 02HQGR0008

February, 2004

Table of Contents

LIST OF FIGURES

ABSTRACT

The Imperial fault is the only fault in southern California to have ruptured in two major earthquakes in the 20th century. In 1940, it ruptured end-to-end (both north and south of the international border) in an M_W 6.9 earthquake, and in 1979, the northern segment of the fault (north of the border) ruptured again in an M_W 6.4 event. Slip in 1940 was highest (5–6 m) along the central portion of the fault and lowest (less than 1 m) along the northern portion, with a high slip gradient between these two segments just north of the border. The 1979 earthquake involved surface rupture along only the northern 30 km of the fault, with dextral offsets being sub-meter and being nearly identical to 1940 offsets along the northern 20 km of the rupture. The similarities and differences of the two events led to the "slip-patch model" for the Imperial fault, whereby the fault ruptures with frequent moderate earthquakes along its northern end, like in 1979, and with less frequent larger events like 1940 along its entire length. According to the model, the central patch, which experienced high slip in 1940 and did not rupture in 1979, would rupture with relatively infrequent events (roughly every 260 years) with typically 5–6 m of slip per event; meanwhile, the northern patch, which corresponds to the 1979 rupture, would rupture more frequently (roughly every 40 years) with up to 1 m of slip per event. This model is consistent with the slip distribution observed in 1940 and in 1979. Paleoseismic investigations along the central patch also support this model, as the penultimate event there occurred at around A.D. 1700, shortly after the last Lake Cahuilla highstand. Prior to the present investigation, however, there were no data on events prior to 1940 on the northern patch, which could serve to either support or refute the slip-patch model.

We have opened a trench across the Imperial fault south of Harris Road, adjacent to Mesquite Basin, where the fault has both dextral and normal slip components. On the downdropped side of the

fault, a laminated clay unit (inferred to be the most recent Lake Cahuilla clay, at ca. A.D. 1680) is exposed in the trench and is overlain by more than 1.5 m of younger deposits; the overlying material consists of bedded fine sands and silts (inferred to be overbank deposits from a nearby channel), which interfinger with massive silty clays (inferred mostly to be colluvium). Unfortunately, the normal component of slip for all earthquakes in the trench was almost exclusively restricted to a single east-dipping plane or set of closely spaced planes, so that the amount of dip slip per event cannot be accurately resolved; nonetheless, a series of fissures and flower structures adjacent to the main fault in the hangingwall block permit the distinction of individual events. There is good evidence for three events and weak evidence for a fourth event on the northern Imperial fault since the last Lake Cahuilla highstand, based on filled-in fissures and abrupt upward terminations of multiple fault strands and liquefaction cracks. The youngest of these events are inferred to be 1979 and 1940; the oldest, which produced liquefaction and ruptured to the top of the most recent lake deposits, probably occurred very soon after the peak of the last highstand, based on the arguments that no lake deposits post-date the event, and that the ground was still saturated at the time of the earthquake. This event may have been the penultimate (ca. A.D. 1700) event seen on the central patch of the Imperial fault at the international border. The other event seen in our trench (the one for which there is only weak evidence) produced much less deformation, and we cannot preclude the possibility that it was only triggered slip, resulting from an earthquake on a nearby fault. If it was an earthquake on the northern Imperial fault, it may have been the April 1906 M 6.1 Imperial Valley event, or one or both of a pair of nearly identical M ~6 events in the southern Imperial Valley in June 1915; alternatively, it may have been a 1979-type event, following the ca. A.D. 1700 event by several decades. We see no evidence in our trench for regularly repeating 1979-type events as suggested by the slip-patch model. We propose an alternative model, in

which the northern portion of the Imperial fault normally ruptures less frequently than every 40 years, with higher amounts of slip than experienced in 1940 and 1979. In this model, the short interval between the 1940 and 1979 events can be explained by the high slip gradient at the international border in the 1940 earthquake—with slip of less than 1 m to the north ramping up sharply southward to more than 5 m of slip in the region of the border—which simply reloaded the northern portion of the fault and hastened the time until it failed again.

INTRODUCTION

The northwest striking, dextral Imperial fault comprises one of the main structural elements of the San Andreas fault system in the Salton Trough of southern California (Lomnitz *et al.*, 1970; Elders *et al.*, 1972; Sharp, 1982a; see Figure 1). The fault is approximately 70 km long, terminating at major right steps located at the Salton Buttes and Cerro Prieto geothermal fields, both of which are characterized by high heat flow and dense microseismicity (Lomnitz *et al.*, 1970). The Imperial fault is the only fault in southern California to have ruptured twice in the 20th century. However, the ruptures were not self similar or "characteristic." The fault ruptured end-to-end in an M_W 6.9 earthquake in 1940, producing surface rupture over its entire length (Buwalda and Richter, 1941; see Figure 1). The rupture nucleated along the northern third of the fault in or just south of Mesquite Basin (Buwalda and Richter, 1941; Doser, 1990), with most of the rupture propagation directed to the southeast. In the region of nucleation, surface slip was measured at less than a meter, but it quickly increased southward to ~6 m south of Heber dunes, was ~5 m at the international border, dropped to ~2.7 m near Tamaulipas (historically, Cucapa), and terminated near Saltillo at the step-over between the Imperial and Cerro Prieto faults. Thirty-nine years later, the Imperial fault again produced surface rupture in the 15 October 1979 M_W 6.4 earthquake (Sharp, 1982b). This time, however, subsurface slip nucleated south of the international border and ruptured unilaterally northwestward beneath the zone of 1940 high surface slip, producing surface rupture only northwest of Heber dunes along the northern third of the fault (see Figure 1); the

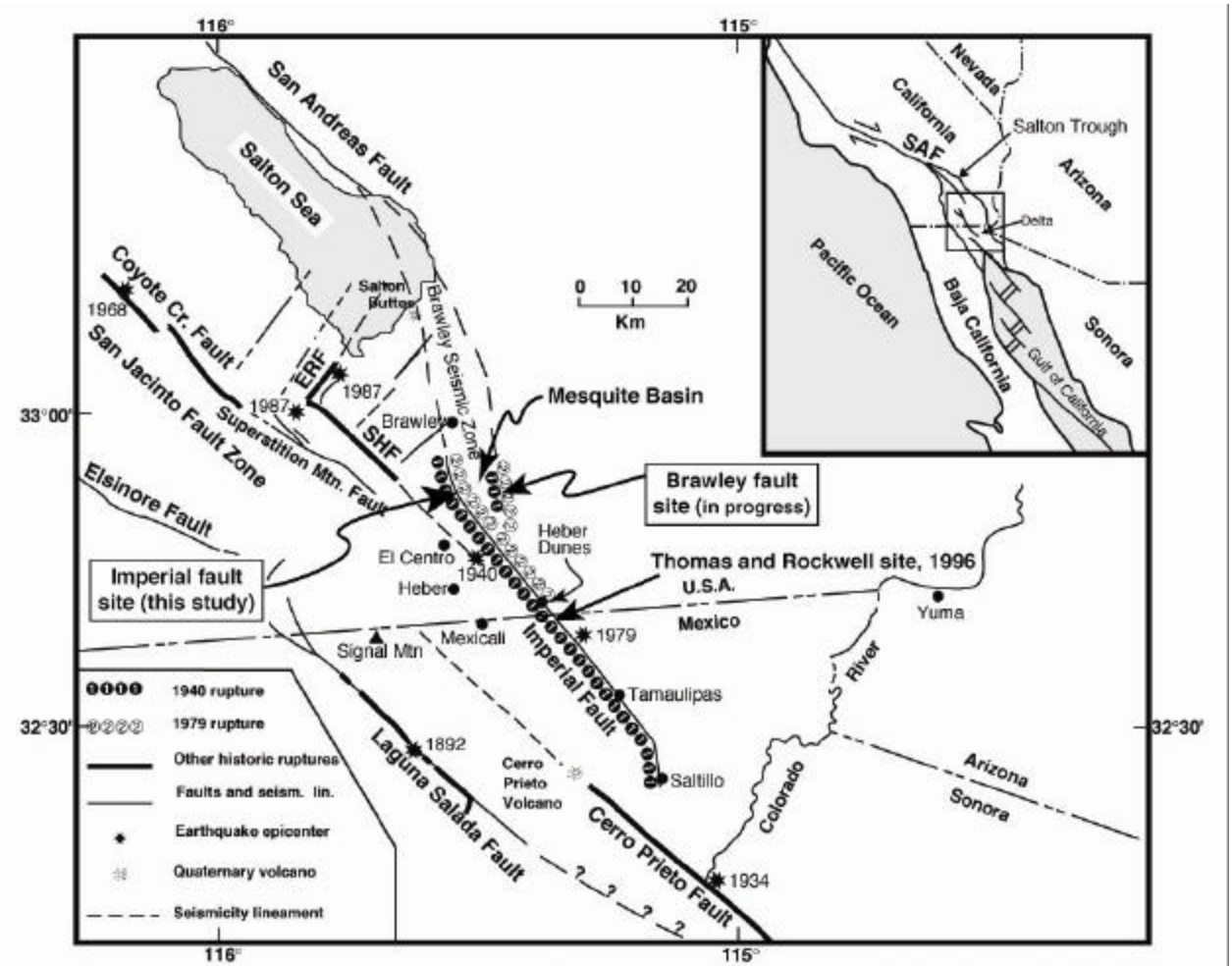

Figure 1. Generalized fault map of the southern part of the Salton Trough. Surface ruptures indicated for the 1892 (M 7 1/4), 1934 (ML 7.1), 1940 (MW 6.9), 1968 (MW 6.5), 1979 (MW 6.4), and 1987 (MW 6.2 and 6.6) earthquakes.

southeastern terminus of 1979 slip corresponded to where slip had begun to ramp up in 1940 (Archuletta, 1984). Surface slip in 1979 reach a maximum of ~70 cm, similar to that for the northern third of the fault in 1940, and the areas of highest slip in 1979 coincided with the areas of highest slip along the northern segment in 1940.

It is clear that these two earthquakes were not characteristic, and Sieh (1996) used this pattern of locally similar surface slip in dissimilar earthquakes to argue for a "slip-patch" model of earthquake behavior (Figure 2). In this model, the Imperial fault is divided into three "slip patches" that each fail with their own characteristic slip. The northern Imperial segment is a slip patch that characteristically

ruptures with 0.5–1 m of slip and simply re-failed in 1979 due to strain accumulation along the fault. In this scenario, relatively frequent earthquakes will rupture the northern Imperial fault roughly every 40–70 years (Sieh, 1996) to make up the slip deficit along that portion of the fault, which experiences less slip when the entire fault ruptures, as in 1940, every 250 years or so (Thomas and Rockwell, 1996). As Sieh (1996) noted, the gradual, nearly identical, northward decline in dextral slip during both earthquakes is probably a long-term characteristic of the Imperial fault, because the northern 15 km of the fault forms the southwestern boundary of a large dilatational stepover; thus, the northward diminutions of dextral slip in 1940 and 1979 are probably manifestations of a gradational tectonic transfer of slip across the dilatational stepover. Nonetheless, as Sieh (1996) further pointed out, the great difference in slip between the northern and central portions of the fault cannot be explained by the tectonic stepover, and no large geometrical complexity or additional active structure exists far enough south along the Imperial fault to explain the slip gradients seen a few kilometers north of the international border. In general, the slip-patch model predicts that segmented faults will tend to fail in segments with similar amounts of slip, regardless of the rupture direction, state of stress, or amount of slip propagating into the segment. Sieh (1996) and others (*e.g.*, Anderson and Bodin, 1987) have suggested that poorly located events in 1906 and 1915 may have occurred on the northern patch of the Imperial fault, although neither event has been attributed to a particular fault by paleoseismic methods, and prior to this study, essentially nothing was known about the pre-1940 earthquake history of the northern Imperial fault.

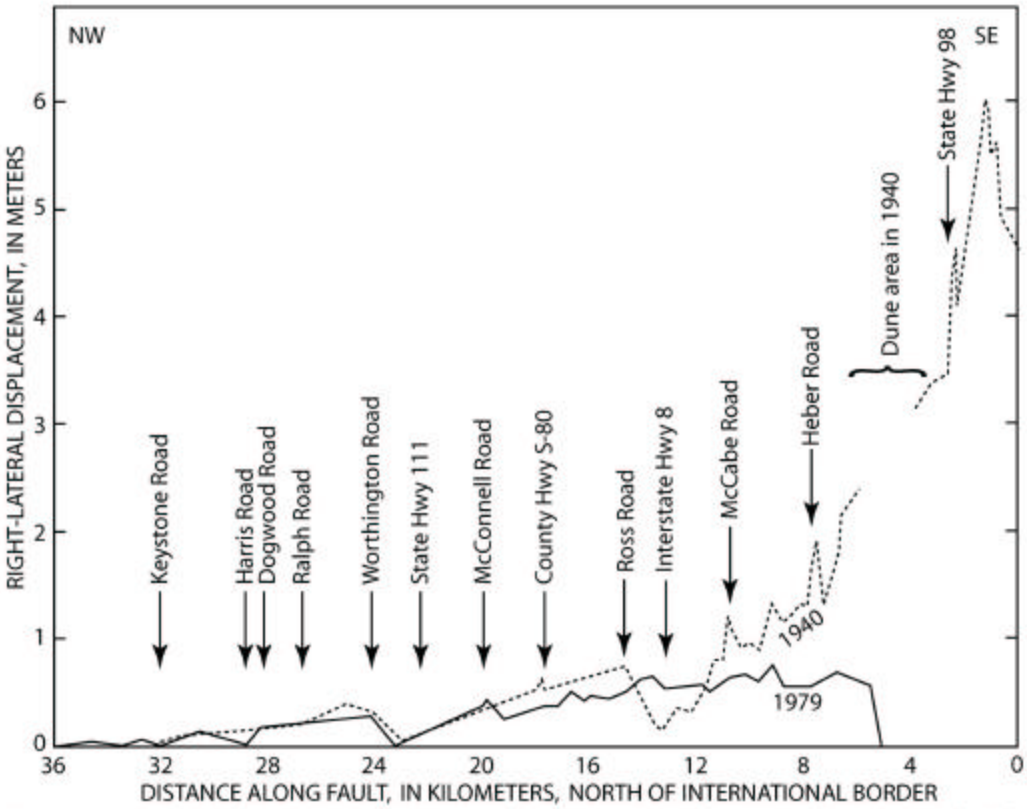

Figure 2. (a) Profiles of right-lateral component of displacement as a function of length along fault for the 1940 and 1979 ruptures. Comparison of slip in the two events shows important similarities and differences. Sieh (1996) argued that this example supports the concept of characteristic slip within individual patches of a fault, but not characteristic earthquakes. He argued that the sharp slip gradients in both 1940 and 1979 a few kilometers north of the international border suggest the presence of a fixed patch boundary. Redrafted from Sharp (1982b).

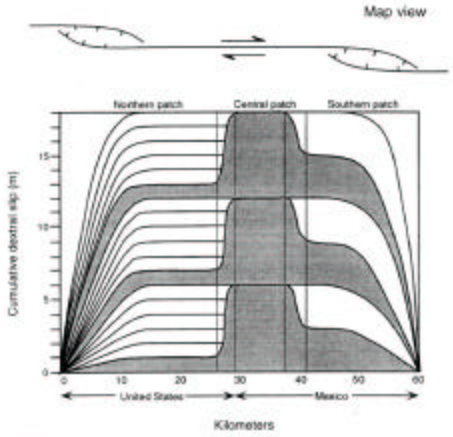

Figure 2b

(b) Diagram illustrating the "slip-patch" model as proposed by Sieh (1996) for the Imperial fault: accumulated over scores of earthquake cycles, slip along the fault between stepovers is uniform, and in both stepover regions, slip tapers to zero. According to the model, each of the three patches along the fault has its own characteristic slip function, and narrow transition zones separate these regions of characteristic slip. From Sieh (1996).

Because of the abundance of historical earthquakes that could be attributed to the Imperial fault and the two known historical surfaces ruptures in 1940 and 1979, the Imperial fault is assumed to have a very short repeat time. Furthermore, it is assumed to take most or all of the geodetically measured slip between Cerro Centinela and Yuma, about 40 mm/yr, which also would predict a short recurrence interval (Savage *et al.*, 1979; Lisowski *et al.*, 1991; Larsen and Reilinger, 1992). This contrasts with the paleoseismic observations of Thomas and Rockwell (1996) along the central Imperial fault at the international border, in the area where the fault failed with 5 m of slip in 1940: they observed evidence for only one other surface rupture during the past 320 years. The prior event there occurred at around A.D. 1700, shortly *after* the peak of the ca. A.D. 1680 highstand of Lake Cahuilla, perhaps only years after the most recent event along southernmost San Andreas fault that was documented by Sieh and Williams (1990) to have occurred *during* the peak of that highstand.

We propose an alternative model whereby the initial slip pulse in 1940 nucleated with a relatively small displacement of less than a meter in the north (Doser, 1990) and then ramped up to 5–6 m south of Heber dunes (Sharp, 1982b; Thomas and Rockwell, 1996). According to this model, the large displacement (~6m) in the vicinity of the international border (Thomas and Rockwell, 1996), and the high slip gradient immediately to its north, reloaded the northern Imperial fault, which subsequently re-failed in 1979 to accommodate the lesser amount of slip along that section in 1940. Presumably, if in the previous 1940-type event in about A.D. 1700 slip was low along the northern portion of the fault, the ca. 1700 event may have been followed by a 1979-type event along that northern portion of the fault. Alternatively, if the ca. 1700 rupture had propagated from south to north, and if the slip distribution in that event was more evenly distributed than in 1940, then the ca. 1700 event may be the only prehistorical event during the past 320 years along the central or northern Imperial fault.

Our work involved an attempt to shed light on some of these questions. We excavated a trench across the Imperial fault south of Harris Road, adjacent to Mesquite Basin, to gain information about the behavior of the northernmost third of the Imperial fault over the past few centuries. We herein present the results of our trenching effort, which do not support a "slip-patch" model for this fault. Indeed, the close timing of the two historical events seems anomalous in context of the behavior of the fault over the last few hundred years. Although a single trench at any site is rarely enough to understand the complete slip history of a fault over a period of time, our trench at this site is enough to distinguish between the two models just discussed, and it will be useful for determining where and how future efforts at the site should be directed.

THE IMPERIAL FAULT AT HARRIS ROAD

Because of vigorous agricultural activity in this region, nearly the entirety of the surface trace of the northern Imperial fault has been graded, and many geomorphic features have been and continue to be obliterated, but a comparatively pristine section of fault is preserved adjacent to Mesquite Basin between Dogwood and Harris Roads (see Figures 3 and 4). Although there are motorcycle tracks and evidence of off-road vehicle usage over most of the site, the site itself has not been plowed. The upper few tens of centimeters (presumed to represent deposition in the past few decades, based on the fact that these units overlie the most recent historical faulting event or are just below the most recent event horizon) appear to have been distorted under the weight of off-road vehicles, but there is no evidence that any of the section has been removed by anthropogenic means such as plowing, except possibly in a few isolated locations. Earlier historical deposits that postdate the 1940 earthquake (*i.e.*, that overlie the penultimate event horizon) generally appear undisturbed.

The 1940/1979 scarp is well-expressed along this section of the fault, with 1940 and 1979 slip superposed on a preexisting scarp. The overall scarp height exceeds 2.5 m and it is not clear how much of this is post-lake slip, but the lake deposits appear to have been draped across a preexisting scarp.

The overall trend of the Imperial fault is to the northwest and the sense of slip is predominantly dextral, although adjacent to Mesquite Basin along the fault's northernmost stretch, there is also an extensional east-side-down component. Indeed, Mesquite Basin is a structural graben, bounded by the oblique northwest trending Imperial fault on the west, and by the oblique north trending Brawley fault on the east. Locally, in the vicinity of Harris Road, the Imperial fault strikes approximately north (see Figure 3).

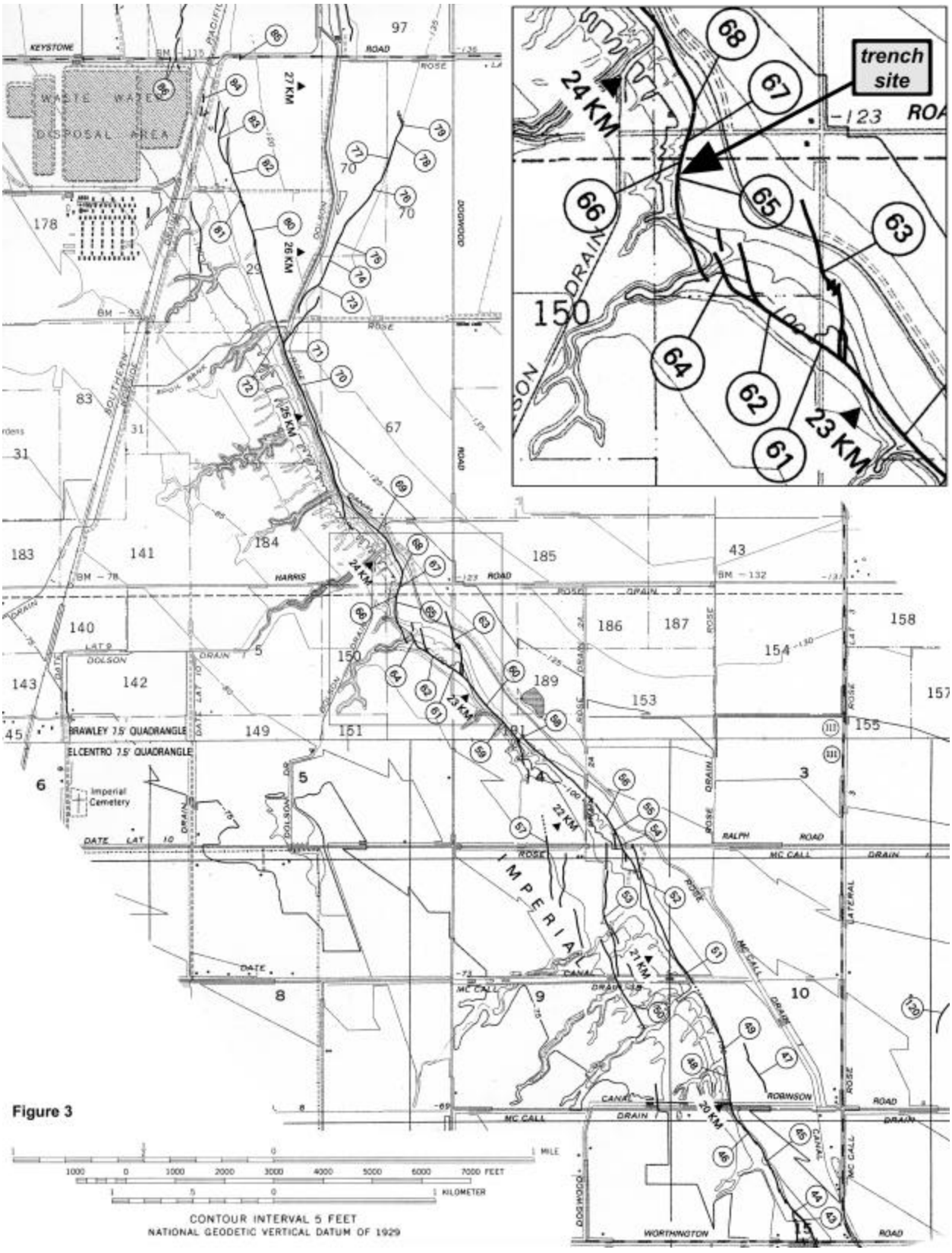
trench site
24 KM
23 KM
68
67
66
65
64
63
62
61
150
DRAIN
ROAD
IMPERIAL
CONTOUR INTERVAL 5 FEET
NATIONAL GEODETIC VERTICAL DATUM OF 1929

Figure 3

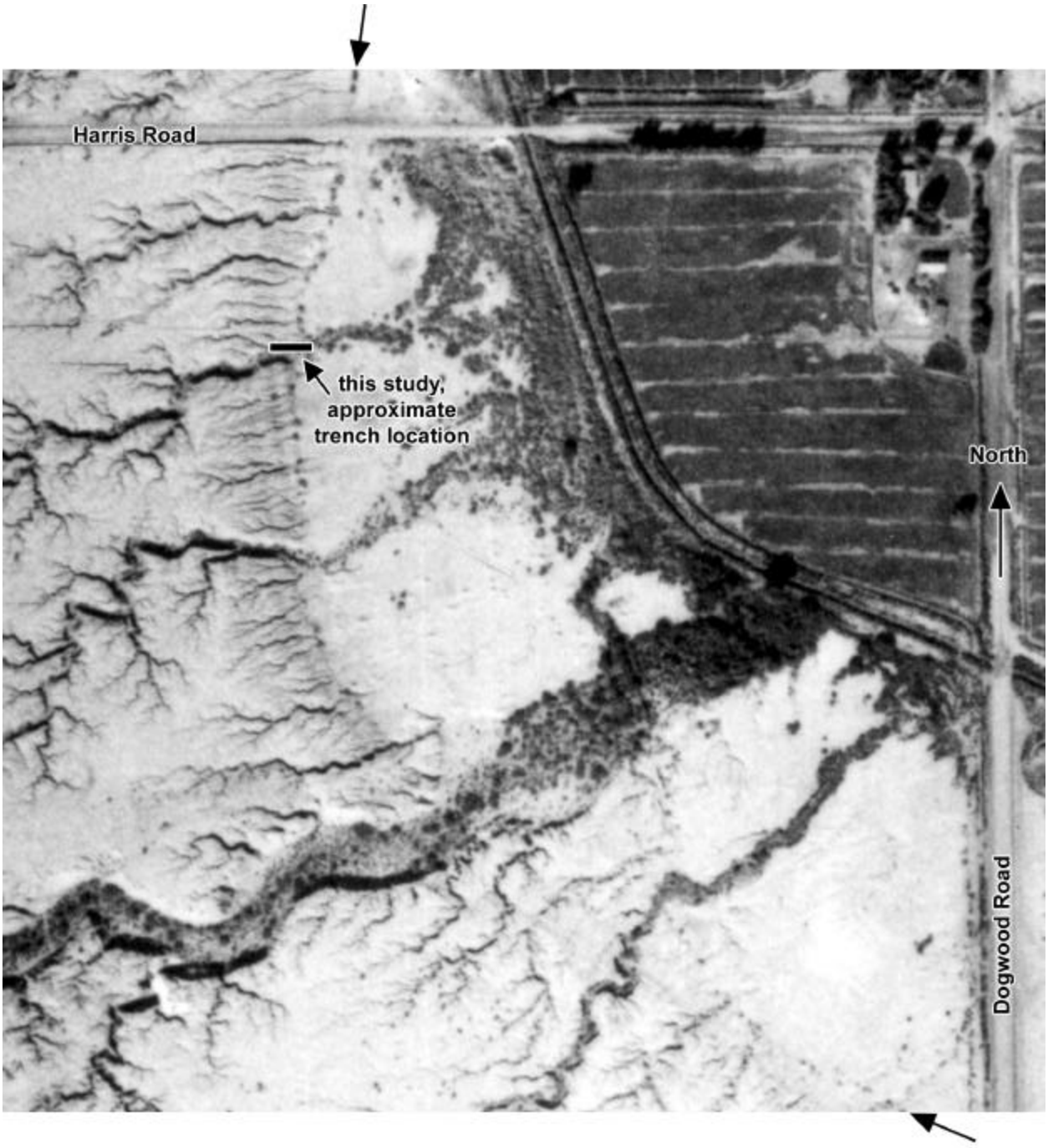
Harris Road
this study,
approximate
trench location
North
Dogwood Road

Figure 4a

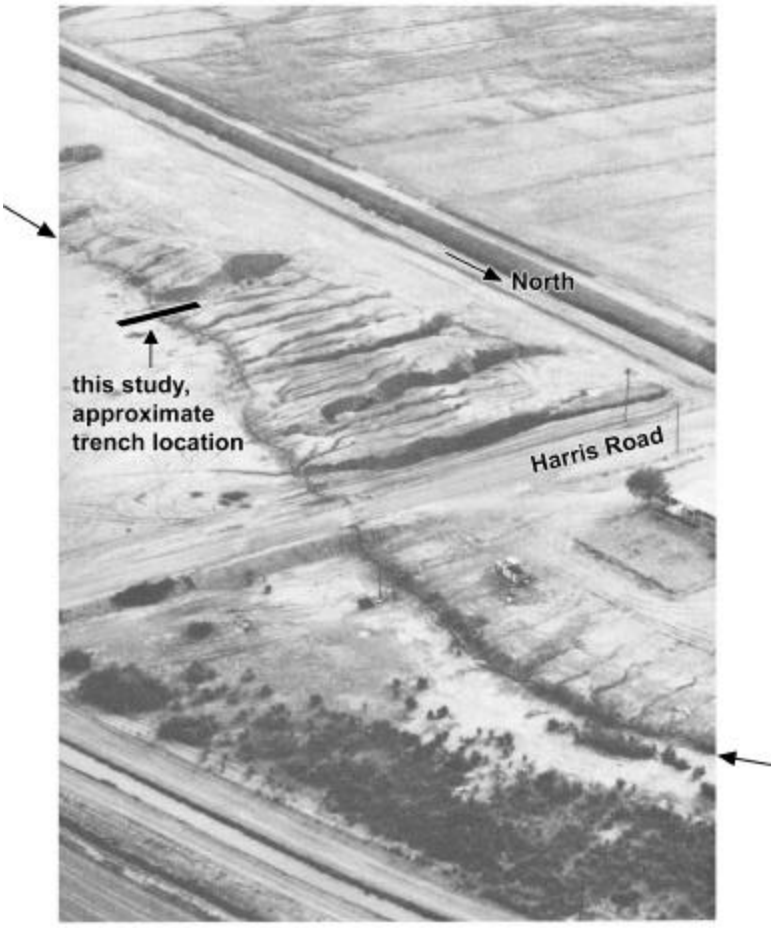

FIGURE 4b—Imperial fault at Harris Road (loc. 67), which passes between utility poles on right. Sinuosity of fault trace is typical of much of northern segment of Imperial fault where vertical component of slip is large. Gullying of upthrown (southwest) side of fault has etched rounded late Holocene scarp. Note general but imperfect congruence of new surface rupture (dark narrow line) with base of older escarpment. View southwestward. Photograph by M. J. Rymer, October 23, 1979.

Following the 1940 earthquake, the nearest offset measurement was along Harris Road, where ~15 cm of dextral slip and ~25 cm of east-side-down dip slip were recorded 13 days after the mainshock (J. P. Buwalda, unpub. field notes, 1940). In 1979, slip in the vicinity of the trench site was predominantly vertical, with dip separations of 16-28 cm and negligible lateral slip recorded by Sharp *et al*. (1982). Measurements of slip at several locations in the vicinity of the trench site following the 1940 and 1979 earthquakes are given in Table 1. In contrast with the small amount of cumulative lateral slip in the past two earthquakes, several small channels show prominent right-lateral deflections, which are inferred to be the result of appreciable lateral slip in events prior to 1940. Hence, 3-dimensional trenching at the Dogwood site will eventually be required to test for the longer-term slip vector, and to resolve the size of earlier events. Nonetheless, a 2-dimensional trench, which was excavated, logged, and interpreted for this study, has been very instructive in answering our first-order questions.

METHODOLOGY

A single trench was excavated perpendicular to the Imperial fault on an undeveloped, unplowed lot south of Harris Road and west of Dogwood Road. The trench was situated several meters northwest of the thalweg of a small channel incised into the footwall of the fault. We chose the location so as to be near the channel—with the anticipation that bedded channel deposits would provide better event resolution than massive colluvial deposits—while avoiding both the incised upslope portion of the channel and its offset downstream counterpart, to preserve those for future 3-dimensional trenching. Because of access issues, the trench was dug to a depth of only 2.5 m, but that was sufficiently deep to expose the strata down to and below the most recent Lake Cahuilla deposits. Both walls of the trench were gridded, etched, and photographed. The photographs were mosaicked together and rectified to the grid, and field logging was done directly on the rectified mosaicked photographs. The drafted logs are shown in Figure 5.

The initial chronology of stratigraphic units was established based on the principle of superposition and the seemingly irrefutable assumption that the uppermost sequence of laminated clay deposits belong to either the A.D. 1680 highstand of Lake Cahuilla or to an earlier lake (historical evidence precludes a significant lake at any time more recent than the early 18th century; see Sieh and Williams, 1990). The initial chronology was supported by results of ^{14}C analysis using accelerator mass spectrometry (AMS) techniques on individual pieces of detrital charcoal from various strata. Historical deposits were also recognized in some cases by the inclusion of in situ historical debris, such as glass shards.

TRENCH STRATIGRAPHY

Regionally, for the last millennium and presumably longer, sedimentation in the Imperial Valley has been cyclic and dominated by the Colorado River. At least five times in the past 1000 years, the Colorado River has switched from its present course (emptying southward into the head of the Gulf of California) to flowing northward, directly into the Salton Trough. Each time the Colorado River followed a northward course, it inundated much of the Coachella and Imperial Valleys, producing the freshwater Lake Cahuilla that typically rose to elevations of between 9 and 13 m above modern sea level (Stanley, 1963, 1966; Thomas, 1963; Van de Kamp, 1973; Waters, 1983; Sieh, 1986; Sieh and Williams, 1990; Rockwell and Sieh, 1994; Gurrola and Rockwell, 1996; Thomas and Rockwell, 1996). After filling to an elevation of 13 m, any additional water would "spill out" of the basin and flow southward into the Gulf of California; eventually, the Colorado River would then revert to a southward course, and due to the hot, dry climate, Lake Cahuilla would desiccate in a matter of 60–70 years (Sieh and Williams, 1990). While five Lake Cahuilla highstands have been recognized in the past 1000 years at various sites along the shoreline (see references above), it is possible that there were additional partial fillings of the lake in which the Colorado River did not flow northward for a long enough duration to fill the lake entirely. In the early 20th century, attempts to divert part of the Colorado River into the Imperial Valley for agricultural purposes resulted in the entirety of the Colorado River flowing uncontrolled into the Salton Trough for two years, from 1905 to 1907. The Salton Sea, as it was then called, reached a maximum elevation of 60.2 m below sea level in February 1907 (Sykes, 1937, Figure 62) before it was brought under control, and it remains at about –70 m today.

Sub-aqueous deposits that have typically been associated with Lake Cahuilla range from deltaic sands to lacustrine clays. Deltaic deposits may originate from the Colorado River, or they may have a

more local source if a large storm that caused significant runoff along the basin margins occurred while Lake Cahuilla was stationary at a particular level. Lacustrine deposits may also originate locally or from the Colorado River and represent deeper water settling of suspended load. Other deposits in the Imperial Valley typically derive from sources at basin margins and include alluvial fans, braided streams, and barrier beaches. Sands from both sources have been reworked into extensive aeolian deposits (Van de Kamp, 1973).

The Imperial fault site at Harris Road sits at an elevation of 33.5 m below sea level. This elevation places the site well below the Lake Cahuilla shoreline, but well above the 1907 highstand of the Salton Sea. The uppermost ~1.5 m of the trench exposure on the downdropped side of the fault consists of a sequence of laminated to bedded silty fine sands interbedded with occasional irregular chunky clay units (Units 10–170; see Figure 5). The source of the sandy units is not clear, but several possibilities exist. The trench lies adjacent to a small channel that is eroded headward into the fault scarp, and although some of the sands may be overbank deposits derived from this channel (especially those that have been deposited during the historical period, since the late 19th century), the channel appears too small to be responsible for the entirety of the deposits. Some of the older sands in the uppermost 1.5 m may be derived from the New River. An inspection of a topographic map generated from DEM imagery (Figure 6; from D. Ragona, SDSU, unpublished MS thesis) reveals that the Imperial fault site at Harris Road sits on the margin of a prehistoric New River delta that must have formed when an ancient Lake Cahuilla was stable at this level. (The delta, which extends from –20 m to –40 m [see Figure 6], is too high in elevation to be associated with the 1905–1907 filling of the Salton Sea.)

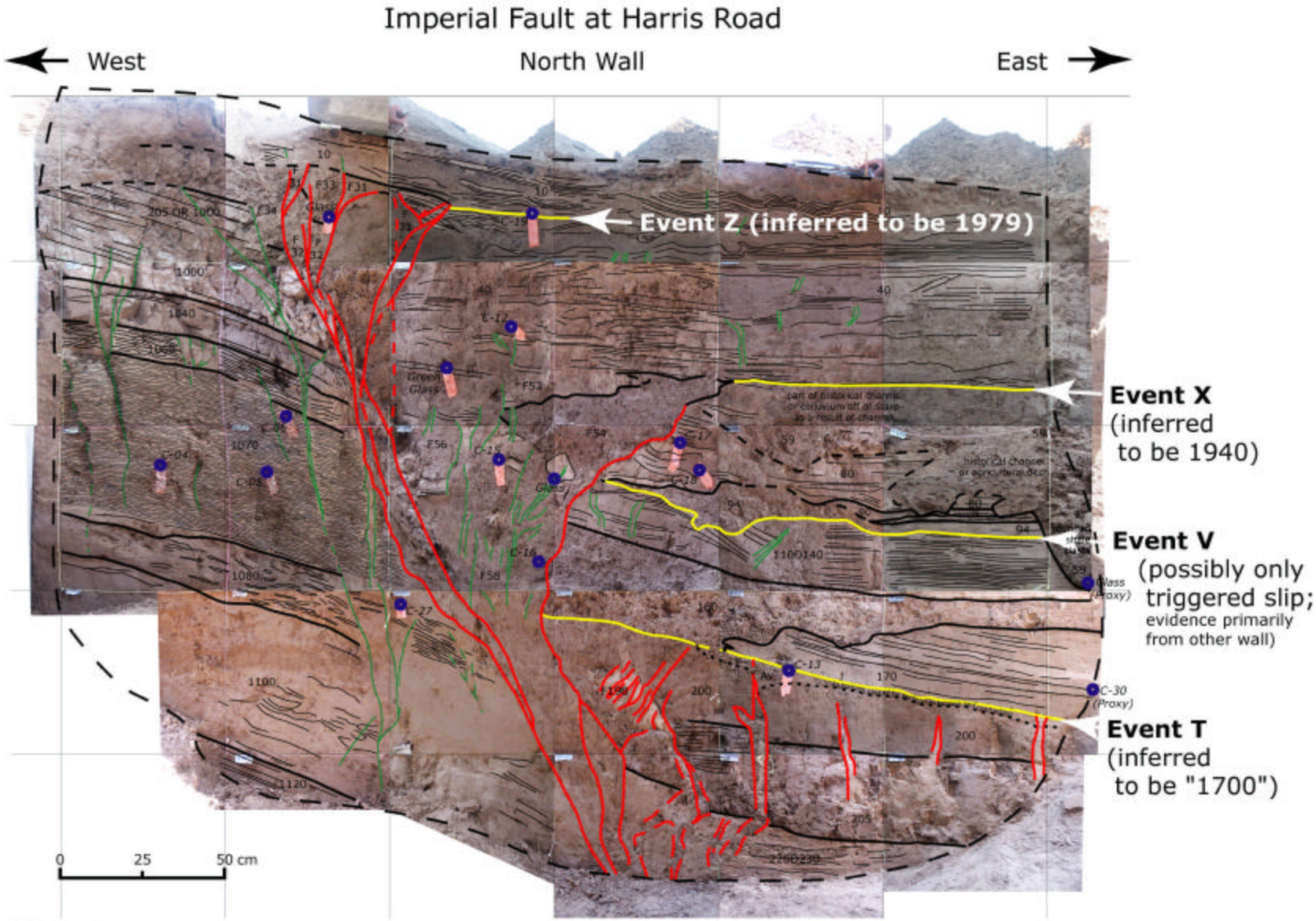

Figure 5a Portions of the logs of the north wall of the trench. Units numbered 240 and lower are inferred to have been deposited in the last 500–1000 years; units numbered 1000 and higher (in the footwall / upthrown block) may be several thousand years old. Carbon-14 sample sites are denoted by open circles.

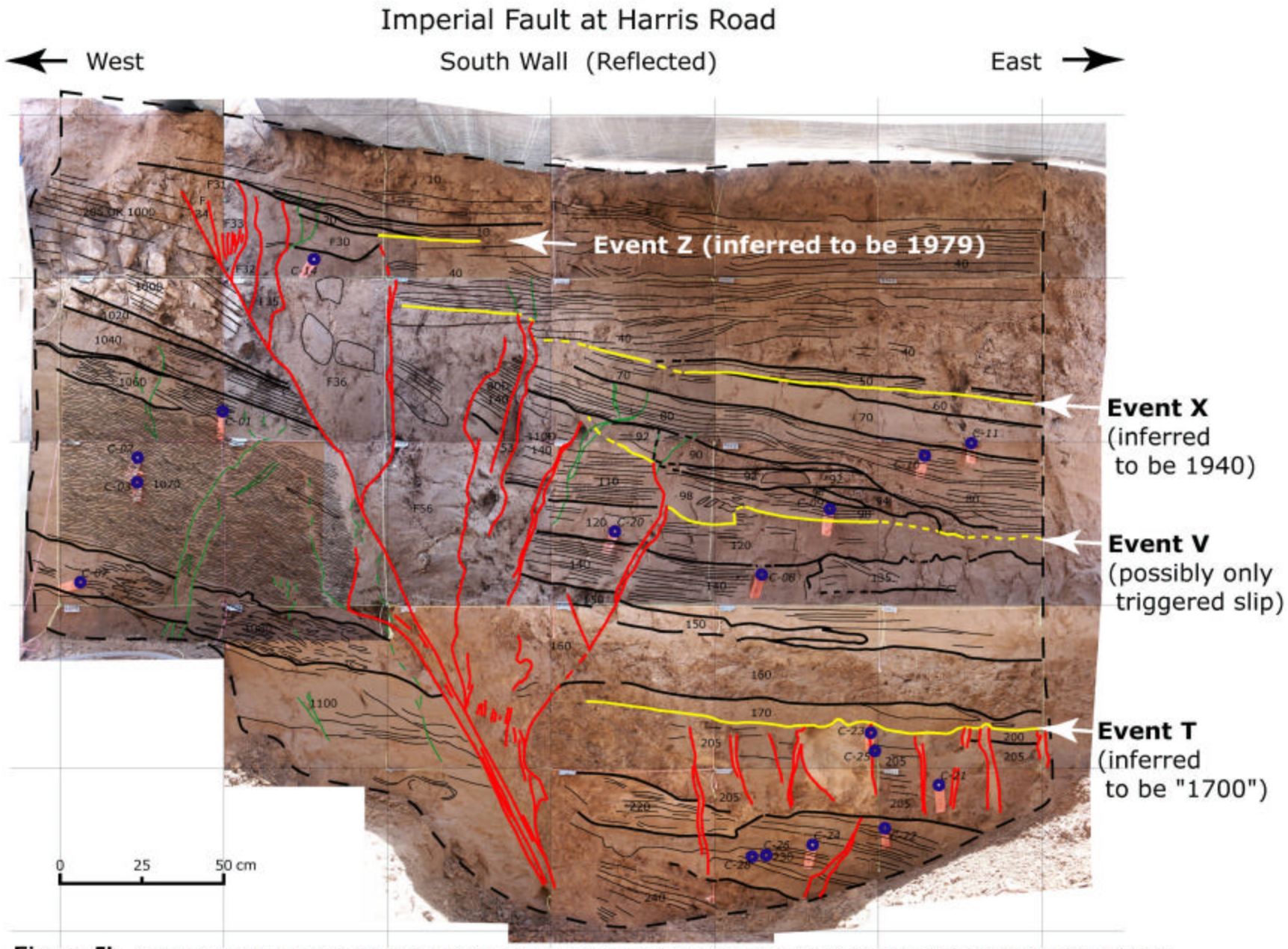

Figure 5b Portions of the logs of the (reflected) south wall of the trench. Units numbered 240 and lower are inferred to have been deposited in the last 500–1000 years; units numbered 1000 and higher (in the footwall / upthrown block) may be several thousand years old. Carbon-14 sample sites are denoted by open circles.

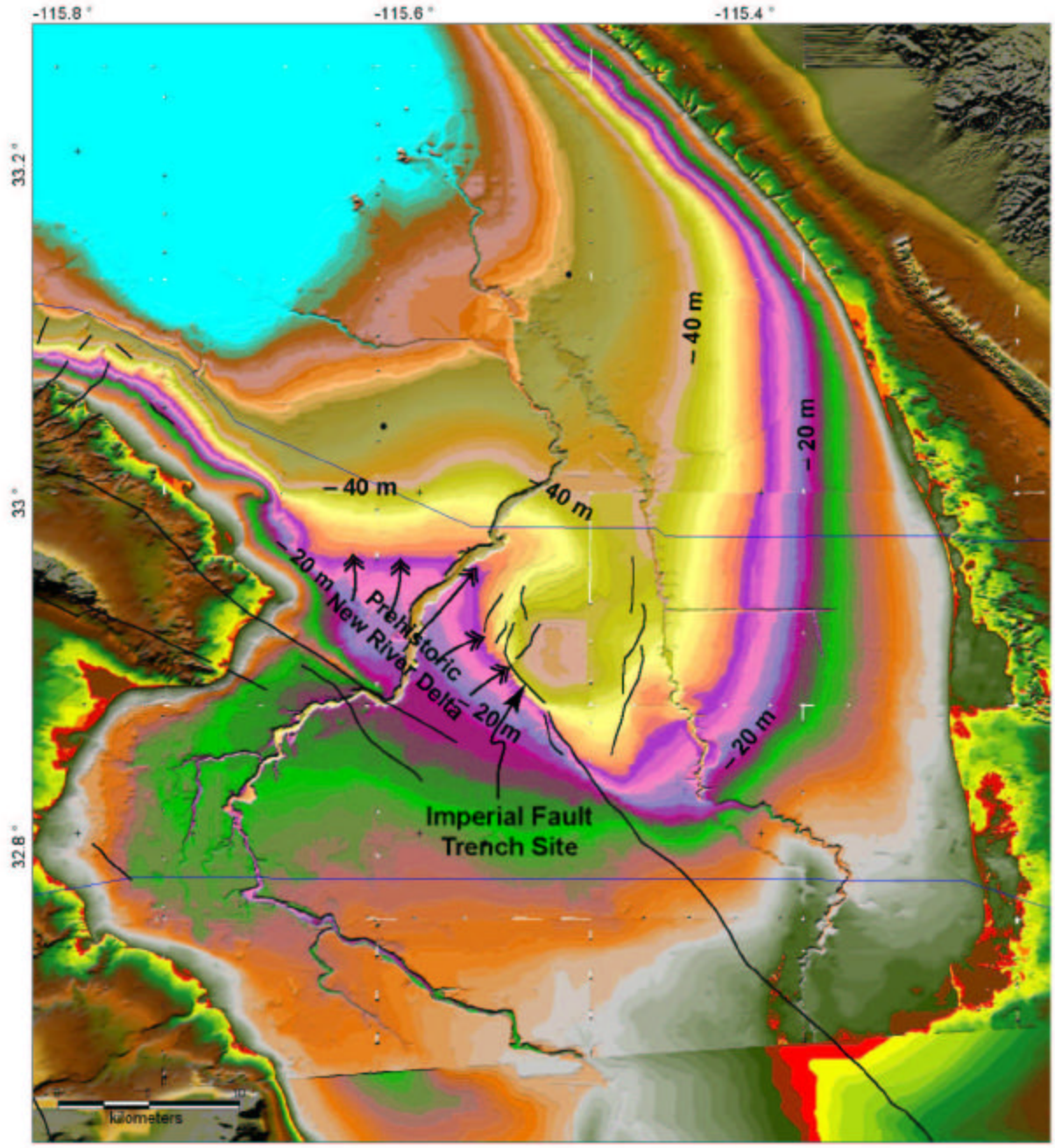

Figure 6 DEM image of the Imperial Valley, showing the Imperial and Brawley faults, the trench site, and a prehistoric New River delta that must have formed during an ancient Lake Cahuilla stillstand. Adapted from an unpublished MS thesis by D. Ragona.

The timing of this delta is not well constrained; all we know is that it must predate the historical period, during which there is no record of a stillstand of Lake Cahuilla at this level, yet it must be young enough to still be recognizable in the present topography. Based on these conditions and available information, it must predate the most recent highstand in A.D. 1680. After that time, historical accounts by Spanish explorers and oral traditions by the native Cahuilla preclude a significant highstand.

The other distinct set of deposits in the uppermost 1.5 m of the downdropped side consists of irregular "chunky" clays. These units are characteristically poorly sorted and not laminated. While the modal grain size of these units is clay, the clay itself occurs in coarse sand–sized and larger fragments and is mixed with silt and fine sand. We infer that these units represent colluvium derived predominantly from laminated clay units exposed upslope in the free face of the fault scarp. Some of these irregular clay units might be interpreted as being wedge-like in shape, but others appear to have a more uniform thickness and still others have irregular, probably erosional contacts.

Underlying the uppermost 1.5 m of silty fine sands and chunky clays is a sequence of clay deposits (Units 200–205; see Figure 5) interpreted to be lacustrine in origin and further inferred to represent the most recent Lake Cahuilla highstand, dated by Sieh and Williams (1990) to have occurred at ca. A.D. 1680. [All the radiocarbon dates from this trench, which are presented in Table 2, are from detrital charcoal. While they are consistent with the age of the clay deposits being ca. A.D. 1680, they do not provide an entirely robust constraint on that age: they only constrain the clays to be younger than ca. A.D. 1300. From historical evidence, Sieh and Williams (1990) precluded the possibility of a Lake Cahuilla highstand at any time more recent than ca. A.D. 1680; although the sparse early historical data might permit a short-lived partial filling of Lake Cahuilla more recently than ca. A.D. 1680 (and prior to the 20th century), the substantial thickness (~25 cm) of the laminated clay (Unit 205) requires that the

trench site be submerged for a substantial period of time. Thus, Unit 205 cannot be younger than ca. A.D. 1680. It is conceivable that Units 200–205 are as old as A.D. 1300, but the lack of any younger lacustrine deposits and the lack of signs of significant erosion strongly suggest that, at the very least, Units 200–205 include the ca. A.D. 1680 lake clays. For now, we will assume that Units 200–205 represent only the ca. A.D. 1680 lacustrine deposits; in the Discussion, we will comment on the potential impact there might be on our conclusions if in fact Units 200–205 partially or wholly represent older lakes.] The lower portion of the lacustrine clay deposits are finely laminated and grayer in color, while the upper portion is more massive in nature and browner in color. Because of the fine grain size and the laminations, the unit is interpreted to represent pulses of sedimentation in a relatively deep-water environment. It is not clear why the laminations do not continue to the top of the clay, but it could be a result of bioturbation or it could represent a different process of subaqueous sedimentation. Below the lacustrine clays is another sequence of bedded sand deposits that were only partially exposed (Units 220–240).

On the upthrown side of the fault, the stratigraphic sequence is generally disparate (again, see Figure 5). The uppermost ~20 cm has been greatly disturbed, either by biogenic or anthropogenic causes, and is very loose; it is difficult to recognize any bedding in this zone, and it is impossible to ascertain the mode of emplacement of these sediments. Below the uppermost disturbed zone is a sequence of finely laminated gray clay (Units 1000–1040) that appear similar to, but are substantially thicker than, the laminated lacustrine clay (Unit 205) that is near the base of the trench on the downdropped side. No part of Unit 1000 can plausibly be younger than Unit 205, because that would require net deposition on the upthrown side of the fault during the same time period that there was net erosion of the downdropped side, which would be contrary to expected deposition patterns.

Furthermore, because of the clay's greater thickness on the upthrown side, the entirety of Unit 1000 cannot be the same age as Unit 205. We infer either (a) that Unit 1000 represents the cumulative deposition of multiple lakes (possibly including the most recent lake), with no net non-lacustrine deposition between the lakes, or (b) that it represents a prior filling of Lake Cahuilla, in which case either the lake was full for a longer duration, or the sedimentation pattern was different. Depending upon which scenario is correct, the most recent (ca. A.D. 1680) lacustrine clay may or may not be preserved at the very top of Unit 1000, but, regardless, the base of Unit 1000 must be older than Unit 205. The one radiocarbon sample from the footwall constrains the upthrown clays to be younger than ca. 1500 B.C. (Table 2).

Below the uppermost lacustrine clays on the upthrown side lies a sequence of cross-bedded very fine sandy silts (Unit 1060), which are underlain by a sequence of cross-bedded clayey silty fine sands (Unit 1070); the cross-bedded silts and sands are inferred to be fluvial or deltaic in origin. The cross-bedded clayey silty fine sands are underlain by a distinctive sequence of sharply interfingering gray silty clay and orange-brown fine sand (Unit 1080), and this distinctive unit is in turn underlain by a sequence of faintly cross-bedded silt and very fine to fine sand (Unit 1100). Aside from possibly the laminated lacustrine clay deposits (Unit 205), none of the units exposed in the hangingwall appear to be present in the footwall exposure.

STRUCTURE AND EARTHQUAKE HISTORY

We have uncovered good evidence for four events since the deposition of the youngest lacustrine clays, based on filled-in fissures and abrupt upward terminations of multiple fault strands and liquefaction cracks. For discussion purposes, we refer to the events, in order of increasing age, as Events Z, X, V, and T, respectively (see Figure 5).

Event Z: The primary evidence for Event Z consists of a large fissure (units F30 through F36; see Figure 5) at the same horizon on both walls. It is overlain by very loose bedded silty fine sands. The fissure has clearly been re-faulted since it was filled in, and a few cracks extend upward into the overlying bedded material; these observations are consistent with aseismic creep and triggered slip that has been documented at the site and in the vicinity since 1979 (*e.g.*, Louie *et al.*, 1985; Sharp *et al.*, 1986). This is the most recent event in the trench, so it must represent, at least in part, the 1979 earthquake.

Event X: The primary evidence for Event X also consists of a large fissure (units F52 through F58; see Figure 5) at the same horizon on both walls. It is overlain by bedded silty fine sands. The fissure has clearly been re-faulted since it was filled in, and a few cracks extend upward into the overlying bedded material; these observations are consistent with aseismic creep that has been documented at the site since the 1970s. That this event is historical (since the early 20th century) is demonstrated by a piece of anthropogenic glass found at the base of the filled-in fissure (north wall, Figure 5a, Unit F54).

Event V: Although the relative amount of slip in this event cannot be determined from our study, Event V produced an order of magnitude less apparent ground deformation than Events Z or X, which may indicate that it was a smaller event; alternatively, the deformation might have been triggered slip caused by an earthquake on a nearby fault, a phenomenon that has been observed historically numerous times on faults in the Imperial Valley. The primary evidence for Event V consists of several faults that appear to have significant (though small) apparent vertical separation below the event horizon (top of Unit 110), whereas, above the event horizon, either they do not continue, or they appear to simply be cracks, with negligible displacement; these faults appear only on the south wall (Figure 5b). On both walls of the trench, this event horizon is overlain by a package of deposits (Units 90–98) that looks colluvial either in composition or overall shape, or both. While the date of this event is not well constrained, it may be the elusive source of the 1906 *M* 6.1 "Brawley" earthquake that followed the 1906 San Francisco earthquake by 11 hours (see Meltzner and Wald, 2003), or it may be one or both of a pair of nearly identical *M* ~6 events in the Imperial Valley in June 1915 (see Beal, 1915; Anderson and Bodin, 1987; and Toppozada and Branum, 2002).

Event T: The primary evidence for Event T consists of multiple upward terminations of liquefaction cracks which pervasively deform the uppermost Lake Cahuilla clay (Units 200–205), but which are overlain by unfaulted bedded stratigraphy (Unit 170) and a thick layer of "chunky" clay (Unit 160) that is inferred to be colluvial in origin (that is, gravity-derived from immediately up-slope) (see Figure 5). Interestingly, most of the liquefaction cracks do not appear to be rooted; instead, most of the cracks deform only the lacustrine clay, and there is no measurable vertical displacement across most of them. We infer there to have been a detachment at the base of the laminated clay, and we infer that while the

strike-slip faulting passed relatively "cleanly" through the underlying units as simple dextral motion, the clay deformed as rigid blocks that rotated to accommodate the lateral motion; as the blocks of clay rotated, cracks opened between them, and liquefied sand from underlying units used the tensile cracks as upward conduits. We observed that most of the liquefaction cracks were at random oblique angles to the overall trend of the fault, with angles ranging from near parallel to near perpendicular.

We base our interpretation of the timing of Event T on several observations at this site, and on our knowledge of the timing of events at other sites in the region. Foremost, we infer from the occurrence of liquefaction at this site that the ground was saturated (under water or very shallow water), but we infer from the fact that some of the liquefaction cracks extend to the top of the laminated clay that the lake was in its waning stage (i.e., it was after the peak of the high stand), as there was no deep-water deposition (settling of suspended load) after Event T. Together, these observations and inferences suggest that Event T occurred several years to several decades after the peak of the highstand (which is inferred, as discussed earlier, to be the ca. A.D. 1680 highstand). Additional evidence for our interpretation of the timing comes from the appearance of what is inferred to be either a wetting/drying surface or a thin Av soil horizon on top of the laminated clay, suggesting that the surface was briefly exposed to air soon after event T. Finally, the apparent delay after the event before the deposition of colluvium suggests that the earthquake occurred when the site was under water, and that the scarp was preserved (and mostly uneroded) until it was subaerially exposed (again, perhaps years to a few decades later).

In comparison to events at other sites in the region, this event would have necessarily post-dated the most recent event along the southernmost San Andreas fault at Indio, which clearly occurred during the peak of the last Lake Cahuilla highstand (Sieh and Williams, 1990), but Event T coincided

(within temporal resolution) with the penultimate event along the Imperial fault at the international border, which deformed the beach deposits overlying the most recent lacustrine clay deposits; the international border site is just below the Lake Cahuilla shoreline, so the event at the border necessarily occurred at least a few years after the peak of the most recent Lake Cahuilla highstand (Thomas and Rockwell, 1996).

DISCUSSION

This study documents evidence for four earthquakes and afterslip on the northern Imperial fault since deposition of the ca. A.D. 1680 clay. Unfortunately, the normal component of slip for all earthquakes in the trench was almost exclusively restricted to a single east-dipping plane or set of closely spaced planes, so that the amount of dip slip per event cannot be resolved; nonetheless, a series of fissures and flower structures adjacent to the main fault in the hangingwall block permit the distinction of individual events. The two most recent events are unambiguously historical and are inferred to be the 1940 and 1979 earthquakes. The earliest of these events necessarily occurred soon after deposition of the ca. A.D. 1680 clay, and it is inferred to be the same event as the penultimate event (ca. A.D. 1700) seen on the Imperial fault at the international border (Thomas and Rockwell, 1996). This leaves only one event (Event V) that was documented in our trench that could have occurred between the ca. A.D. 1700 event and 1940. It is certainly clear that slip in Event V was minor in comparison to the more recent ruptures. It is important to note that the evidence for Event V is not strong, and what we are calling Event V may only be triggered slip caused by an earthquake on a nearby fault. If that is the case, then there is no evidence for events between the ca. A.D. 1700 event and 1940.

Earlier we discussed the possible age of Units 200–205, the clay deposits inferred to represent the most recent Lake Cahuilla highstand. We argued that Unit 205 cannot be younger than ca. A.D. 1680, but we recognized that all or part of Units 200–205 may be as old as A.D. 1300, based on the moderate constraints of the radiocarbon samples. For the purpose of the discussion that followed, we assumed that Units 200–205 represent only the ca. A.D. 1680 lacustrine deposits; if, however, the only sedimentation during the period A.D. 1300 to 1680 was in the form of laminated clays (*i.e.*, if there was no fluvial, deltaic, or subaerial deposition during that time) or if there was substantial unrecognized

erosion of the downthrown side of the fault at any time since A.D. 1680, then Units 200–205 may partially or wholly represent lakes prior to the ca. A.D. 1680 highstand (as early as A.D. 1300). If only part of Units 200–205 represent the ca. A.D. 1680 lake, and the rest represents prior lakes, our history of earthquakes on the northern Imperial fault since A.D. 1680 does not change. If Units 200–205 wholly represent prior lakes, then event T may have occurred prior to A.D. 1680, and there is evidence for at most three events (which include 1940 and 1979) since A.D. 1680.

If Sieh's (1996) "slip-patch" model is appropriate for the Imperial fault, there should be evidence for moderate (0.5–1 m) slip events on the northern Imperial fault roughly every 40–70 years (Sieh, 1996); in other words, there should be evidence for 3–5 events between ca. 1700 and 1940, not including the ca. 1700 and 1940 events themselves. Instead, we see evidence for at most one event in that period, and it appears to be small. While it is possible in almost any trench to be missing one or more events (which is why it is generally good practice to examine multiple exposures at any site), the extensive ground deformation caused in our exposures by the 1979, 1940, and ca. 1700 earthquakes makes it implausible that we are missing 2 or more events between ca. 1700 and 1940. Nonetheless, more work is warranted at this site to explore the possibility of there being events missing from our exposures.

We propose an alternative model whereby the initial slip pulse in 1940 nucleated with a relatively small displacement of less than a meter in the north (Doser, 1990) and then ramped up to 5–6 m south of Heber dunes (Sharp, 1982b; Thomas and Rockwell, 1996). According to this model, the large displacement (~5m) in the vicinity of the international border (Thomas and Rockwell, 1996), and the high slip gradient immediately to its north, reloaded the northern Imperial fault, which subsequently re-failed in 1979 to accommodate the lesser amount of slip along that section in 1940. Presumably, if in

the ca. A.D. 1700 event slip was low along the northern portion of the fault (as in 1940), then the ca. 1700 event may have been followed by a 1979-type event along only the northern portion of the fault. (Event V may be this event.) Alternatively, if the ca. 1700 rupture had propagated from south to north, and if the slip distribution in that event was more evenly distributed than in 1940, then the ca. 1700 event may have been followed by 200–240 years of quiescence along the central and northern Imperial fault. More work is warranted at this site to attempt to constrain the 3-D slip history of the fault, and to attempt to determine slip per event. Of course, the model we are proposing and the slip-patch model are end-member models, and reality may lie somewhere in between.

CONCLUSIONS

There is good evidence for three events and weak evidence for a smaller fourth event on the northern Imperial fault since the last Lake Cahuilla highstand, based on filled-in fissures and abrupt upward terminations of multiple fault strands and liquefaction cracks. The youngest of these events are inferred to be 1979 and 1940; the oldest, which produced liquefaction and ruptured to the top of the most recent lake deposits, probably occurred very soon after the peak of the last highstand, based on the arguments that no lake deposits post-date the event, and that the ground was still saturated at the time of the earthquake. This event may have been the penultimate (ca. A.D. 1700) event seen on the central patch of the Imperial fault at the international border. The other event seen in our trench (the one for which there is only weak evidence) produced much less deformation, and we cannot preclude the possibility that it was only triggered slip, resulting from an earthquake on a nearby fault. If it was an earthquake on the northern Imperial fault, it may have been the elusive April 1906 *M* 6.1 Imperial Valley event (see Meltzner and Wald, 2003), or one or both of a pair of nearly identical *M* ~6 events in the southern Imperial Valley in June 1915 (see Beal, 1915); alternatively, it may have been a 1979-type event, following the ca. A.D. 1700 event by several decades. We see no evidence in our trench for regularly repeating 1979-type events as suggested by the slip-patch model. We propose an alternative model, in which the northern portion of the Imperial fault normally ruptures less frequently than every 40 years, with higher amounts of slip than experienced in 1940 and 1979. In this model, the short interval between the 1940 and 1979 events can be explained by the high slip gradient at the international border in the 1940 earthquake, which simply reloaded the northern portion of the fault and hastened the time until it failed again. Further work at this site, including 3-dimensional trenching, should help confirm our results and will hopefully elucidate lingering questions about the slip history of the northern Imperial fault.

ACKNOWLEDGMENTS

We thank the many people who have been directly and indirectly involved with this project. Foremost, we thank Danielle Verdugo for help in hand-excavating and deepening parts of the trench and for help in logging a portion of the trench walls. Tom Fumal and Gordon Seitz provided valuable insight into the trench stratigraphy and faulting behavior. Clarence Allen provided unpublished material and advice. Michaele Kashgarian provided speedy results of the analysis of our radiocarbon samples. Daniel Ragona compiled the DEM image we used in Figure 6. This project was funded by NEHRP grant 02HQGR0008.

REFERENCES CITED

Anderson, J.G. and P. Bodin (1987). Earthquake recurrence models and historical seismicity in the Mexicali-Imperial Valley, *Bull. Seism. Soc. Am.* **77**, 562-578.

Archuletta, R.J. (1984). A faulting model for the 1979 Imperial Valley earthquake, *J. Geophys. Res.* **89**, 4559-4585.

Beal, C.H. (1915). The earthquake in the Imperial Valley, California, June 22, 1915, *Bull. Seism. Soc. Am.* **5**, 130-149.

Buwalda, J.P. and C.F. Richter (1941). Imperial Valley earthquake of May 18, 1940, *Geol. Soc. Am. Bull.* **52**, 1942-1943.

Doser, D.I. (1990). Source characteristics of earthquakes along the southern San Jacinto and Imperial fault zones (1937 to 1954), *Bull. Seism. Soc. Am.* **80**, 1099-1117.

Elders, W.A., R.W. Rex, T. Meidav, P.T. Robinson, and S. Beihler (1972). Crustal spreading in southern California, *Science* **178**, 15-24.

Gurrola, L.D. and T.K. Rockwell (1996). Timing and slip for prehistoric earthquakes on the Superstition Mountain fault, Imperial Valley, southern California, *J. Geophys. Res.* **101**, 5977-5985.

Larsen, S. and R. Reilinger (1992). Global Positioning System measurement of strain across the Imperial Valley, California: 1986-1989, *J. Geophys. Res.* **97**, 8865-8876.

Lisowski, M., J.C. Savage, and W.H. Prescott (1991). The velocity field along the San Andreas fault in central and southern California, *J. Geophys. Res.* **96**, 8369-8389.

Lomnitz, C., F. Mooser, C.R. Allen, J.N. Brune, and W. Thatcher (1970). Seismicity and tectonics of the northern Gulf of California region, Mexico: preliminary results, *Geofis. Int.* **10**, 37-48.

Louie, J.N., C.R. Allen, D.C. Johnson, P.C. Haase, and S.N. Cohn (1985). Fault slip in southern California, *Bull. Seism. Soc. Am.* **75**, 811-833.

Meltzner, A.J. and D.J. Wald (2003). Aftershocks and triggered events of the great 1906 California earthquake, *Bull. Seism. Soc. Am.* **93**, 2160-2186.

Rockwell, T.K. and K. Sieh (1994). Correlation of large earthquakes using regional lacustrine stratigraphy, examples from the Salton Trough, California, *Geol. Soc. Am. Abstr. Programs* **26**, A-239.

Savage, J.C., W.H. Prescott, M. Lisowski, and N. King (1979). Deformation across the Salton Trough, California, 1973-1977, *J. Geophys. Res.* **84**, 3069-3079.

Sharp, R.V. (1982a). Tectonic setting of the Imperial Valley region, in *The Imperial Valley, California, Earthquake of October 15, 1979, U.S. Geol. Surv. Profess. Pap. 1254,* 5-14.

Sharp, R.V. (1982b). Comparison of 1979 surface faulting with earlier displacements in the Imperial Valley, in *The Imperial Valley, California, Earthquake of October 15, 1979, U.S. Geol. Surv. Profess. Pap. 1254,* 213-221.

Sharp, R.V. *et al.* (1982). Surface faulting in the central Imperial Valley, in *The Imperial Valley, California, Earthquake of October 15, 1979, U.S. Geol. Surv. Profess. Pap. 1254,* 119-143.

Sharp, R.V., M.J. Rymer, and J.J. Lienkaemper (1986). Surface displacement on the Imperial and Superstition Hills faults triggered by the Westmorland, California, earthquake of 26 April 1981, *Bull. Seism. Soc. Am.* **76**, 949-965.

Sieh, K.E. (1986). Slip rate across the San Andreas and prehistoric earthquakes at Indio, California, *Eos Trans. AGU* **67**, 1200.

Sieh, K. (1996). The repetition of large-earthquake ruptures, *Proc. Natl. Acad. Sci. USA* **93**, 3764-3771.

Sieh, K.E. and P.L. Williams (1990). Behavior of the southernmost San Andreas fault during the past 300 years, *J. Geophys. Res.* **95**, 6629-6645.

Stanley, G.M. (1963). Prehistoric lakes in the Salton Sea Basin, *Spec. Pap. Geol. Soc. Am.* **73**, 249-250.

Stanley, G.M. (1963). Deformation of Pleistocene Lake Cahuilla shoreline, Salton Basin, California, *Spec. Pap. Geol. Soc. Am.* **83**, 165 pp.

Stuiver, M. and H.A. Polach (1977). Discussion: reporting of C-14 data, *Radiocarbon* **19**, 355-363.

Stuiver, M. and P.J. Reimer (1993). Extended ^{14}C database and revised CALIB 3.0 ^{14}C age calibration program, *Radiocarbon* **35**, 215-230.

Stuiver, M. *et al.* (1998). INTCAL98 radiocarbon age calibration, 24,000-0 cal BP, *Radiocarbon* **40**, 1041-1083.

Sykes, G. (1937). The Colorado Delta, *Carnegie Inst. Washington Publ.* **460** and *Amer. Geographical Soc. Spec. Publ.* **19**, 193 pp.

Thomas, A.P. and T.K. Rockwell (1996). A 300-550-year history of slip on the Imperial fault near the U.S.-Mexico border: Missing slip at the Imperial fault bottleneck, *J. Geophys. Res.* **101**, 5987-5997.

Thomas, R.G. (1963). The late Pleistocene 150-foot fresh water beachline of the Salton Sea area, *S. Calif. Acad. Sci. Bull.* **62**, 9-17.

Toppozada, T. and D. Branum (2002). California earthquakes of M = 5.5: their history and the areas damaged, in *International Handbook of Earthquake and Engineering Seismology* (Part A), W.H.K. Lee, H Kanamori, P.C. Jennings, and C. Kisslinger (Editors), Academic Press, San Diego, CA, 793-796 and CD-ROM.

Van de Kamp, P.C. (1973). Holocene continental sedimentation in the Salton Basin, California: a reconnaissance, *Geol. Soc. Am. Bull.* **84**, 827-848.

Waters, M.R. (1983). Late Holocene lacustrine stratigraphy and archaeology of ancient Lake Cahuilla, California, *Quat. Res.* **19**, 373-387.

Table 1a: Slip Measurements from 1940

Site (see Fig. 3)	Distance (m) North of Trench Site along Fault Strike	Slip Component (cm) Dextral	Slip Component (cm) Vertical (East Side Down)	Days after Earthquake
Dogwood Road	–585	~15	~0	13
Harris Road	105	~15	~25	13

From J. P. Buwalda (unpub. field notes, 1940).

Table 1b: Co-seismic and Post-seismic Slip Measurements from 1979

Site # on Fig. 3	Distance (m) North of Trench Site along Fault Strike	Slip Component (cm) Dextral	Slip Component (cm) Vertical (East Side Down)	Days after Earthquake
61	–585	~16.5	9	?
62	–440	7.5	6.5	9
63	~ –500	?	16.5	7
63	~ –500	?	20	25
63	~ –500	?	25	158
64	–290	4.5	6	25
65	–5	~0	16	4
66	25	~0	27.5	25
67	85	?	24.5	7
67	85	?	34.5	158
68	185	14	10	4

From Sharp *et al.* (1982).

Table 2: Radiocarbon Ages Derived From Detrital Charcoal Samples

Sample (1)	Stratigraphic Unit (2)	$\delta^{13}C$ (3)	Uncalibrated ^{14}C Age, Years B.P. (4, 5)	Calibrated Calendric 2σ Max-Min Date Range (6)	Probability (7)
IFH-C-25	205	-25	510 ± 40	A.D. 1319-1352 A.D. 1388-1454	0.131 0.869
IFH-C-24	230	-25	745 ± 40	A.D. 1214-1301 A.D. 1371-1379	0.982 0.018
IFH-C-26	230	-25	845 ± 35	A.D. 1045-1046 A.D. 1057-1087 A.D. 1121-1138 A.D. 1156-1276	0.003 0.062 0.042 0.894
IFH-C-28	230	-25	580 ± 40	A.D. 1300-1372 A.D. 1378-1422	0.649 0.351
IFH-C-06	1070	-25	3185 ± 35	1521-1402 B.C.	1.000

1) All samples were single chunks of charcoal.

2) Stratigraphic units are numbered such that low numbered units are above (younger than) high numbered units.
Unit numbering scheme is current as of 4 Jan 2004.

3) $\delta^{13}C$ values are the assumed values according to Stuiver and Polach (1977).

4) The quoted ^{14}C age is in radiocarbon years using the Libby half life of 5568 years and following the conventions of Stuiver and Polach (1977).

5) Sample preparation backgrounds have been subtracted, based on measurements of samples of ^{14}C-free coal.
Backgrounds were scaled relative to sample size.

6) Uncorrected ^{14}C ages were dendrochronologically calibrated using Calib Rev 4.3 based on Stuiver and Reimer (1993) and Stuiver *et al.* (1998).

7) Relative area under 2σ probability distribution.